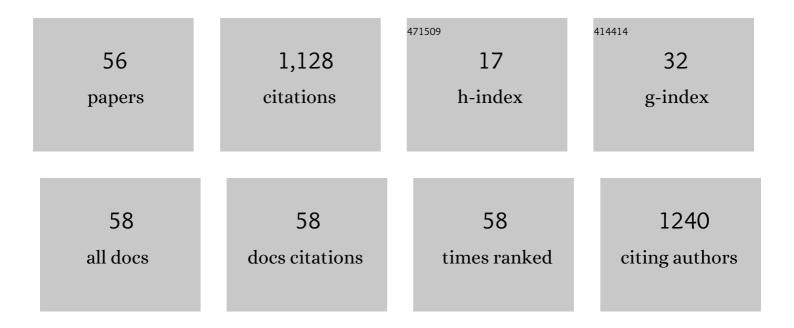
## Mahdi Orooji

List of Publications by Year in descending order

Source: https://exaly.com/author-pdf/7721374/publications.pdf Version: 2024-02-01



#	Article	IF	CITATIONS
1	Perinodular and Intranodular Radiomic Features on Lung CT Images Distinguish Adenocarcinomas from Granulomas. Radiology, 2019, 290, 783-792.	7.3	226
2	Double-Stage Delay Multiply and Sum Beamforming Algorithm: Application to Linear-Array Photoacoustic Imaging. IEEE Transactions on Biomedical Engineering, 2018, 65, 31-42.	4.2	147
3	Linear-array photoacoustic imaging using minimum variance-based delay multiply and sum adaptive beamforming algorithm. Journal of Biomedical Optics, 2018, 23, 1.	2.6	90
4	Double-Stage Delay Multiply and Sum Beamforming Algorithm Applied to Ultrasound Medical Imaging. Ultrasound in Medicine and Biology, 2018, 44, 677-686.	1.5	65
5	A Novel Dictionary-Based Image Reconstruction for Photoacoustic Computed Tomography. Applied Sciences (Switzerland), 2018, 8, 1570.	2.5	57
6	Evaluation of bone regeneration potential of dental follicle stem cells forÂtreatment of craniofacial defects. Cytotherapy, 2015, 17, 1572-1581.	0.7	56
7	Decentralized Hypothesis Testing in Wireless Sensor Networks in the Presence of Misbehaving Nodes. IEEE Transactions on Information Forensics and Security, 2013, 8, 205-215.	6.9	53
8	An integrated segmentation and shape-based classification scheme for distinguishing adenocarcinomas from granulomas on lung CT. Medical Physics, 2017, 44, 3556-3569.	3.0	37
9	Eigenspace-Based Minimum Variance Combined With Delay Multiply and Sum Beamformer: Application to Linear-Array Photoacoustic Imaging. IEEE Journal of Selected Topics in Quantum Electronics, 2019, 25, 1-8.	2.9	33
10	Motion-compensated noninvasive periodontal health monitoring using handheld and motor-based photoacoustic-ultrasound imaging systems. Biomedical Optics Express, 2021, 12, 1543.	2.9	29
11	Brown adipose tissue does not seem to mediate metabolic adaptation to overfeeding in men. Obesity, 2017, 25, 502-505.	3.0	27
12	Quantitative vessel tortuosity: A potential CT imaging biomarker for distinguishing lung granulomas from adenocarcinomas. Scientific Reports, 2018, 8, 15290.	3.3	23
13	Blind Spectrum Sensing Using Antenna Arrays and Path Correlation. IEEE Transactions on Vehicular Technology, 2011, 60, 3758-3767.	6.3	22
14	Improving the Sensing–Throughput Tradeoff for Cognitive Radios in Rayleigh Fading Channels. IEEE Transactions on Vehicular Technology, 2013, 62, 2118-2130.	6.3	22
15	Spectrum Sensing Over MIMO Channels Using Generalized Likelihood Ratio Tests. IEEE Signal Processing Letters, 2013, 20, 439-442.	3.6	21
16	Photoacoustic image formation based on sparse regularization of minimum variance beamformer. Biomedical Optics Express, 2018, 9, 2544.	2.9	20
17	Combination of computer extracted shape and texture features enables discrimination of granulomas from adenocarcinoma on chest computed tomography. Journal of Medical Imaging, 2018, 5, 1.	1.5	20
18	Texture appearance model, a new model-based segmentation paradigm, application on the segmentation of lung nodule in the CT scan of the chest. Computers in Biology and Medicine, 2022, 140, 105086.	7.0	17

Mahdi Orooji

#	Article	IF	CITATIONS
19	Improving Detection Delay in Cognitive Radios Using Secondary-User Receiver Statistics. IEEE Transactions on Vehicular Technology, 2015, 64, 4041-4055.	6.3	16
20	Automatic segmentation of Sperm's parts in microscopic images of human semen smears using concatenated learning approaches. Computers in Biology and Medicine, 2019, 109, 242-253.	7.0	16
21	Medical photoacoustic beamforming using minimum variance-based delay multiply and sum. Proceedings of SPIE, 2017, , .	0.8	10
22	Drug Release Management for Dynamic TDMA-Based Molecular Communication. IEEE Transactions on Molecular, Biological, and Multi-Scale Communications, 2019, 5, 233-246.	2.1	10
23	Validation of delayâ€multiplyâ€andâ€standardâ€deviation weighting factor for improved photoacoustic imaging of sentinel lymph node. Journal of Biophotonics, 2019, 12, e201800292.	2.3	9
24	Dental stem cell banking: Techniques and protocols. Cell Biology International, 2021, 45, 1851-1865.	3.0	9
25	Development of computer-aided model to differentiate COVID-19 from pulmonary edema in lung CT scan: EDECOVID-net. Computers in Biology and Medicine, 2022, 141, 105172.	7.0	9
26	Sparsity-based beamforming to enhance two-dimensional linear-array photoacoustic tomography. Ultrasonics, 2019, 96, 55-63.	3.9	7
27	Automatic Lung Segmentation in Computed Tomography Images Using Active Shape Model. , 2020, , .		7
28	Image enhancement and noise reduction using modified Delay-Multiply-and-Sum beamformer: Application to medical photoacoustic imaging. , 2017, , .		6
29	Photoacoustic Imaging Using Combination of Eigenspace-Based Minimum Variance and Delay-Multiply-and-Sum Beamformers: Simulation Study. , 2017, , .		6
30	A Learning-Based Framework for the Automatic Segmentation of Human Sperm Head, Acrosome and Nucleus. , 2018, , .		5
31	Model-based photoacoustic image reconstruction using compressed sensing and smoothed LO norm. , 2018, , .		5
32	Removing the GSC Noise Reduction deficiencies in Reverberant Environments by Proposing Joint AEC-GSC algorithm. , 2007, , .		4
33	Multi-Antenna Blind Spectrum Sensing for Cognitive Radios Using Path Correlations. , 2011, , .		4
34	Performance analysis of spectrum monitoring for cognitive radios. , 2012, , .		4
35	Segmentation of the pulmonary nodule and the attached vessels in the CT scan of the chest using morphological features and topological skeleton of the nodule. IET Image Processing, 2020, 14, 1520-1528.	2.5	4
36	TDMA-MTMR-Based Molecular Communication With Ligand-Binding Reception. IEEE Transactions on Molecular, Biological, and Multi-Scale Communications, 2021, 7, 111-116.	2.1	4

Mahdi Orooji

#	Article	IF	CITATIONS
37	Intra-perinodular Textural Transition (Ipris): A 3D Descriptor for Nodule Diagnosis on Lung CT. Lecture Notes in Computer Science, 2017, , 647-655.	1.3	3
38	Severity and Progression Quantification of COVID-19 in CT Images: a new Deep-Learning Approach. , 2021, , .		3
39	Molecular Communication Transmitter Design in Limited-Capacity Storage Regime. IEEE Transactions on Nanobioscience, 2023, 22, 212-222.	3.3	3
40	An Unsupervised and Supervised Combined Approach for White Blood Cells Segmentation. , 2018, , .		2
41	Multiple-Type Transmission Multiple-Type Reception Framework on Molecular Communication. IEEE Wireless Communications Letters, 2020, 9, 1825-1829.	5.0	2
42	Distinguishing Adenocarcinomas from Granulomas in the CT scan of the chest: performance degradation evaluation in the automatic segmentation framework. BMC Research Notes, 2021, 14, 87.	1.4	2
43	A simple algorithm to design irregular LDPC codes for finite length. , 2006, , .		1
44	Proposing SVS-PNLMS algorithm for sparse echo cancellation. , 2007, , .		1
45	Spectrum monitoring for cognitive radios in Rayleigh fading channel. , 2012, , .		1
46	Distributed detection in wireless sensor networks in the presence of misbehaving nodes. , 2012, , .		1
47	Evaluating the effects of co-channel interference inwireless networks. , 2013, , .		1
48	Three-dimensional photoacoustic tomography using delay multiply and sum beamforming algorithm. , 2018, , .		1
49	A cluster-based key management framework for resource constraint networks. , 2014, , .		0
50	Spatially aware expectation maximization (SpAEM): application to prostate TRUS segmentation. Proceedings of SPIE, 2014, , .	0.8	0
51	Co-clustering of diseases, genes, and drugs for identification of their related gene modules. , 2016, , .		0
52	Regularized Capon Beamformer Using <tex>\$ell_{1}\$</tex> -Norm Applied to Photoacoustic Imaging. , 2018, , .		0
53	Eigenspace-based minimum variance adaptive beamformer combined with delay multiply and sum: experimental study. , 2018, , .		0
54	Delay-multiply-and-standard-deviation weighting factor improves image quality in linear-array photoacoustic tomography. , 2019, , .		0

#	Article	IF	CITATIONS
55	An advanced sparsity-based photoacoustic image reconstruction algorithm for linear-array transducer scenario. , 2019, , .		0
56	Artifact reduction using minimum variance-based sparse subarray technique in linear-array photoacoustic tomography. , 2019, , .		0